Journal of Polymers and the Environment (2019) 27:2078–2088
https://doi.org/10.1007/s10924-019-01484-1

ORIGINAL PAPER

Enhanced Mechanical and Barrier Performance of Poly (Lactic Acid) Based Nanocomposites Using Surface Acetylated Starch Nanocrystals

Pooja Takkalkar[1] · Gregory Griffin[1] · Nhol Kao[1]

Published online: 19 June 2019

Abstract

Poly (lactic) acid (PLA) based nanocomposites reinforced with starch nanocrystals (SNC) extracted from high amylopectin waxy maize starch and acetylated starch nanocrystals (Ac-SNC), were prepared and their influence on the overall properties of PLA nanocomposites were studied. The two nanofillers (SNC and Ac-SNC) were incorporated in PLA at two different loadings (1 and 3 wt%) by solvent casting and evaporation technique. Surface acetylation of SNC was confirmed by Fourier Transform infra-red spectroscopy and nuclear magnetic resonance spectroscopy and the crystalline structure by X-ray diffraction. This paper reports the influence of incorporating unacetylated and surface acetylated starch nanocrystals on morphological, barrier, mechanical, and rheological properties of PLA based nanocomposites. While both nanofillers improved the properties of PLA, the PLA-Ac-SNC had superior properties to that of PLA-SNC nanocomposites, due to better filler dispersion and interaction with the polymer matrix. These sustainable nanocomposites with improved properties will expand the application of these bio-sourced starch nanocrystals.

Graphical Abstract

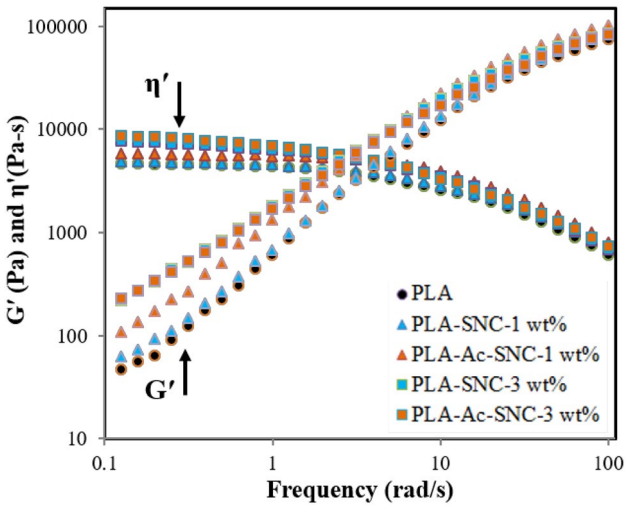

Keywords Polylactic acid · Starch nanocrystals · Acetylation · Nanocomposites · Interfacial interaction

Introduction

There has been increased attention towards developing biodegradable nanocomposites by adding nanofillers, having 1–100 nm dimensions, to bio-based polymers such as polylactic acid (PLA) [1] and polyhydroxybutyrate (PHB) [2] in

✉ Nhol Kao
nhol.kao@rmit.edu.au

[1] Chemical and Environmental Engineering, School of Engineering, RMIT University, Melbourne, VIC 3001, Australia

the past decade. This has been triggered due to the adverse effects posed to the environment due to the extensive reliance on petroleum-based polymers. PLA is obtained from bio-based agricultural resources such as corn and may be processed using commercial processing techniques. However, PLA has certain limitations—narrow processing window and thermal stability, low heat deflection temperature, poor barrier and mechanical properties, etc. which limit its application for use as a replacement for non-biodegradable conventional polymers [3]. There have been previous attempts to overcome these shortcomings of PLA, for instances reinforcing PLA with nanofillers such as cellulose nanocrystals [4–7], starch nanocrystals [8–11], chitin and chitosan nanocrystals [12–14] or plasticizing [15–18]. Reinforcing PLA with polysaccharide nanofillers is gaining significant attention as these nanofillers have the potential to improve the properties of PLA without hindering its biodegradability. In fact they are reported to increase the rate of biodegradation of PLA as the hydroxyl functional groups on the surface of these nanofillers accelerate the rate of hydrolysis of the ester bond [19, 20].

Polysaccharides are categorised as the first and most abundant biopolymers on earth [21, 22]. Among the polysaccharide nanofillers, starch nanocrystals are considered excellent candidates as nanofillers due to their renewability, abundance, biodegradability and ease of processability [23]. Acid, alkaline or enzymatic hydrolysis of starch biopolymer can render rigid structures commonly known as platelet-like starch nanocrystals (SNC). Due to the platelet-like shape of these SNCs they have been studied extensively and are considered to have potential to improve the barrier properties when used as nanofiller in any nanocomposite system [10, 24]. SNC as nanofillers have been incorporated in various polymers such as natural rubber [25, 26], pullulan [27], soy protein [28], waterborne polyurethane [29], starch [30, 31], polycaprolactone [24, 32], and PLA [8–11, 33].

It is challenging to uniformly disperse these nanofillers in a hydrophobic polymer such as PLA, due to the occurrence of hydroxyl functional groups on polysaccharides which limit their miscibility [34]. However it is important to disperse the nanofiller homogeneously in the polymer matrix to achieve superior properties of the nanocomposite [8, 35, 36]. Surface modification is a technique widely used to modify the surfaces of the nanofiller and, basically, replaces the hydroxyl groups with hydrophobic functional groups which helps to disperse the nanoparticles throughout the hydrophobic media. The concept is to control the filler–filler interaction and stimulate the filler-matrix interactions to enhance compatibility and promote good interfacial interaction among the two phases. The different surface treatment approaches for reducing the surface charge of polysaccharide nanofillers include acetylation [37], grafting [8, 9], and silylation [38].

The present study aimed to prepare well-dispersed PLA-SNC and PLA-Ac-SNC nanocomposites at two different loadings (1 and 3 wt%) of each nanofiller (SNC and Ac-SNC) and compare the improvement in properties to that of neat PLA. Further, the effect of surface acetylation of SNC on the overall properties of PLA was investigated. The SNC used in this study was derived from waxy maize starch using a previously reported method by Angellier, Choisnard [39]. To enhance the dispersion of SNC in PLA a surface modification was performed to partly replace the hydroxyl groups on the SNC [40]. The prepared combinations of PLA-SNC and PLA-Ac-SNC nanocomposites were characterized through scanning electron microscopy (SEM) to trace the changes in morphology, Mocon Ox-Tran to estimate the barrier properties in terms of oxygen transmission rate (OTR) and Instron 4467 Universal testing machine to evaluate the mechanical properties through tensile testing. Additionally, to assess the extent of diffusion of the nanofillers in PLA bioploymer the rheological properties were studied through dynamic frequency sweeps tests on the advanced rheometric expansion system (ARES) rheometer.

Statement of Novelty

There have been numerous studies reported on the use of polysaccharide nanofillers such as cellulose and starch to develop the properties of Poly (lactic) acid (PLA) biopolymer. The challenge with development of such hydrophobic PLA based nanocomposites is the difference in polarity, as the polysaccharide nanofillers have hydrophilic characteristics owing to the hydroxyl groups present on their surface. In the present study acetylated starch nanocrystals (Ac-SNC) had been incorporated into PLA, with the intention to disperse them well in PLA as the surface hydrophilicity of Ac-SNC was lower than that of SNC. Although the properties of PLA and starch nanocrystals (SNC) based nanocomposites have been reported previously, the effect of adding Ac-SNC in PLA has not been reported. The PLA-SNC and PLA-Ac-SNC nanocomposites had been characterized for their morphological, barrier, mechanical and rheological properties.

Experimental

Materials

The polylactic acid (PLA) used in this study was procured from NatureWorks (PLA grade- 4032-D) with density 1.24 g/cm^3 and molecular weight 155,000 g/mol. All the analytical grade chemicals including waxy maize starch (99% amylopectin), dichloromethane (DCM), sulfuric acid, glacial acetic acid, acetic anhydride, dimethyl sulfoxide

(DMSO) and ethanol were purchased from Sigma Aldrich and were used as received.

Synthesis of SNCs and Surface Modification

Initially, acid hydrolysis of waxy maize starch using the optimised technique reported by Angellier [39] was employed to prepare SNC. SNC characterization including confirmation of nano-dimensions, shape of SNC, crystalline structure(A-type) and thermal stability by SEM, TEM, XRD and TGA, respectively has been reported in previous work [11]. Furthermore, the prepared SNCs were acetylated using the method reported by Xu [40] with slight modifications. A 5 g sample of freeze-dried SNC with 30 ml of glacial acetic acid was magnetically stirred in a 250 ml round bottom flask. After stirring for 10 min, 60 ml of acetic anhydride was added slowly, followed by a few drops of 0.5 M H_2SO_4. The reactants were stirred at 500 rpm for 5 h at 50 °C. The degree of substitution of SNC was 0.99 when acetylated at 50 °C Xu [40]. Ac-SNC was isolated through precipitation and washed five times with distilled water, followed by two times with 95% ethanol to remove unreacted acetic anhydride and other impurities and then finally freeze-dried for further characterization.

Preparation of PLA-SNC and PLA-Ac-SNC Nanocomposites

Five grams of PLA and the desired amount of SNC or Ac-SNC was dispersed in 50 ml of DCM with constant stirring for 4 h at room temperature. The PLA-SNC and PLA-Ac-SNC nanocomposites were prepared by a solvent casting and evaporating technique. This well-mixed solution of PLA with nanofillers in DCM was transferred onto a glass Petri dish. The nanocomposite films (thickness 0.2 mm) were then peeled off after all the solvent was evaporated overnight. The films were further dried out in a vacuum oven at 40 °C for 24 h to ensure the complete evaporation of remaining DCM. The detailed concentration of SNC and Ac-SNC added in PLA for the present study is shown in Table 1. The samples were labelled as PLA-SNC-1 wt%, PLA-SNC-3 wt%, PLA-Ac-SNC-1 wt% and PLA-Ac-SNC-3 wt%, where the numeral indicated the concentration (wt%) of SNC or Ac-SNC in PLA. The loadings (1 and 3 wt%) of the two nanofillers in PLA were selected based on previous results [11], wherein the optimum concentration of SNC to improve the properties of the nanocomposites was observed around 3 wt%.

Characterization of SNC and Ac-SNC Nanofillers

FT-IR spectroscopic studies of SNC and AC-SNC were done on a PerkinElmer FT-IR spectrophotometer. The scans were recorded in the wavelength range from 4000 to 450 cm^{-1}, 32 scans per sample at a resolution of 4 cm^{-1}. The ^1H NMR spectra were recorded on a Bruker 300 NMR spectrometer with a resonance frequency of 300 MHz. The SNC and Ac-SNC in powder form were dissolved in deuterated dimethyl sulphoxide (DMSO-d6) at room temperature prior to recording the proton NMR spectra. Thermogravimetric measurements of SNC and Ac-SNC were performed using a STA 6000, Perkin-Elmer Instrument, under an instrument air flow of 20 ml min^{-1}. The nanofillers were heated from 30 °C to 600 °C at a heating rate of 10 °C min^{-1} and were stabilised for two minutes at initial and final temperatures. Three replicates were used to characterize each sample, and sample weight percentage was plotted as a function of temperature. XRD patterns were attained by means of a Bruker D4 Endeavor X-ray diffractometer in the angular range of 6–90° (2θ) at a voltage of 40 kV and current of 35 mA. To identify the variations in crystalline structure, if any, after acetylation, peak intensities were recorded every 0.02° at sweep rates of 1.01 2θ min^{-1}.

Table 1 Sample compositions

	PLA (wt%)	SNC (wt%)	Ac-SNC (wt%)
PLA	100	–	–
PLA-SNC-1 wt%	99	1	–
PLA-Ac-SNC-1 wt%	99	–	1
PLA-SNC-3 wt%	97	3	–
PLA-Ac-SNC-3 wt%	97	–	3

Characterization of PLA-SNC and PLA-Ac-SNC Nanocomposites

Morphological Study

FEI Quanta 200 ESEM was used to examine the fractured morphologies of the PLA-SNC and PLA-Ac-SNC nanocomposites. The SEM images were attained at 20 kV accelerating voltage, at 2000 × magnification, under high vacuum mode. The nanocomposite samples were sputter coated with gold, to control charging. For TEM analysis (JEOL 1010), the nanocomposite samples were ultra-microtomed to obtain 100–110 nm thick sections using the Leica UCT Ultra microtome.

Oxygen Permeability

The oxygen transmission rate (OTR) of the nanocomposite films was measured according to the ASTM D-3985 standard in a Mocon OX-TRAN 2/20. The test films were conditioned

in the testing cell prior to testing for 10 h. During the tests the sample were exposed to 0% relative humidity at room temperature with gas flow of 10 ml min^{-1}. Multiple tests were performed and the average results are reported.

Mechanical Testing

Tensile properties of the nanocomposites which included tensile strength (σ_b), Young's modulus (E_{Young}), and elongation at break (ε_b) were measured with an Instron 4467 Universal testing according to ASTM D638. All tests were done using a cross-head speed of 5 mm/min and gauge length of 40 mm at ambient conditions. All the stated values were attained by averaging over five specimens for each set of nanocomposites.

Shear Rheology

Rheological studies of the nanocomposites were performed on a strain-controlled Advanced Rheological Expansion Systems (ARES-TA instruments) rheometer. The nanocomposites rheological properties were studied by means of a force transducer with a parallel-plate fixture of 25 mm diameter and a torque range of 0.2–200 g-cm at 170 °C. Zero gap calibrations at 170 °C were ensured prior to each test. Linear viscoelastic regions (LVR) of nanocomposites were confirmed by conducting the strain sweep tests at a frequency of 1 rad/s and 0.1–100% strain. To understand the influence of SNC and Ac-SNC incorporations on storage modulus (G') and dynamic viscosity (η′) of the nanocomposites, dynamic frequency sweep tests were then done on fresh samples in the LVR with frequency range 0.1–100 rad/s.

Results and Discussion

Acetylation of SNC

Acetylation of SNC had been confirmed by FT-IR and ^{1}H NMR spectrum. Figure 1a shows the FT-IR spectra of SNC and Ac-SNC. The Ac-SNC showed a new band at 1750 cm^{-1}; this was assigned to the C=O ester stretching vibration, which indicated that the acetylation had been successful. In comparison to SNC, the Ac-SNC showed distinct peaks at 1372 cm^{-1} and 1239 cm^{-1} which were attributed to CH_3 symmetrical deformation vibration and carbonyl C–O stretching vibration, respectively [37, 40]. The presences of new peaks after acetylation were an indication that Ac-SNC products were formed through the esterification process [41].

Figure 1b represents the NMR spectra of SNC and Ac-SNC to trace the differences among the two nanofillers clearly. The acetyl groups were substituted on the surface of SNC via the esterification process. The signals due to protons of methyl group appeared at 1.8 to 2.2 ppm [40]. With acetylation new peaks were traced at 5.26, 5.18, 4.76, and 4.22–4.32 ppm, assigned, to the H-3, H-1, H-2, and H-6,60 signals, respectively of the acetyl group on Ac-SNC, which confirmed the successful modification of SNC [40].

Furthermore, the influence of the surface acetylation on the crystalline structure of SNC was inspected by means of XRD analysis. The XRD diffraction patterns of SNC and Ac-SNC are shown in Fig. 1c. The typical diffraction peaks for A-type crystalline starch at 2θ = 15°, 23° and dual peak at 17–18° were apparent for both the SNC and Ac-SNC [11, 42, 43], indicating that the crystalline structure was intact after acid hydrolysis [44] and surface modification. While the intensities of the peaks were reduced slightly for Ac-SNC due to substitution of some hydroxyl groups, the 2θ peaks were still comparable to SNC. Similar results were observed in the case of cellulose nanocrystals and acetylated cellulose nanocrystals [37].

PLA-SNC and PLA-Ac-SNC Nanocomposites Results

Morphological Study

Figure 2a–e shows the fractured surface of the neat PLA, PLA-SNC and PLA-Ac-SNC nanocomposites at different loadings (1 and 3 wt%) of SNC and Ac-SNC nanofiller. The morphology of the nanocomposites was examined by means of SEM to understand the influence of incorporating SNC and the effects of surface acetylation of SNC on the microstructure of PLA. The neat PLA (Fig. 2a) presented a striated and reasonably smooth fractured surface [2, 37, 45, 46]. The unmodified SNC in PLA (Fig. 2b, c) showed a rougher morphology. This indicated that the unmodified SNC had a tendency to agglomerate due to hydrogen bonding and the film forming process used here was not strong enough to control this from occurring. This observation is in a good agreement with that of Fortunati [47] and Fortunati [48]. The rougher surfaces of PLA-SNC nanocomposites indicated the brittleness within these nanocomposites when compared to neat PLA. Furthermore, as the concentration of SNC increased the surface roughness also increased, i.e. the fractured surface of PLA-SNC-3 wt% was rougher than PLA-SNC-1 wt%. The nanocomposites with surface treated SNC showed a different morphology as compared to the nanocomposites with unmodified SNC. The PLA-Ac-SNC nanocomposites appeared to have better and homogeneous dispersion of Ac-SNC in PLA, underlining the positive effect of acetylation of SNC (Fig. 2d, e). When comparing the nanocomposites with surface modified SNC to the unmodified SNC, the acetylated nanocomposites even at higher loading, i.e. PLA-Ac-SNC-3 wt% (Fig. 2e), showed a comparatively smooth surface relative to the PLA-SNC-3 wt%. This indicated that the acetylation process was able

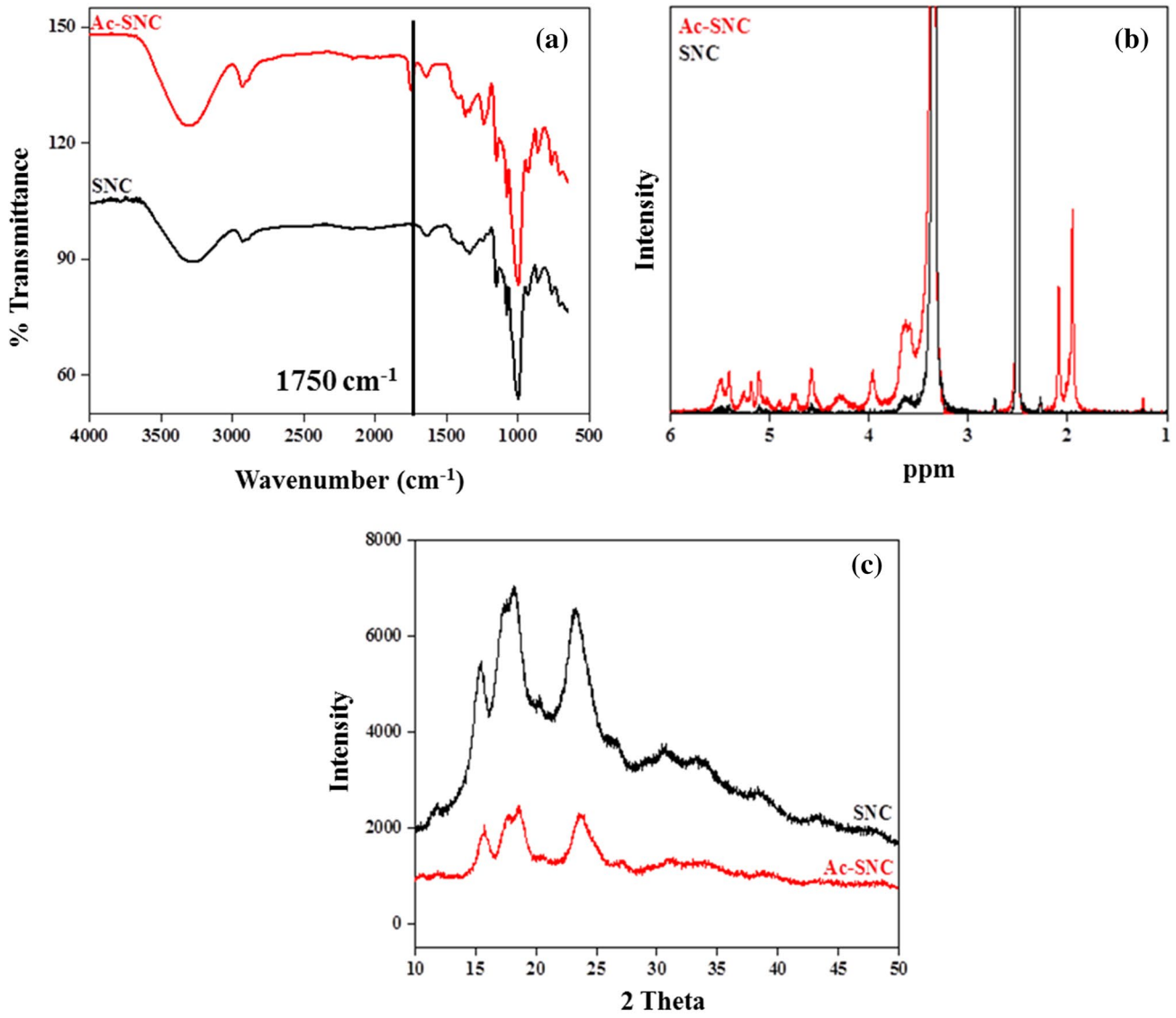

Fig. 1 **a** FT-IR spectra, **b** NMR spectra, and **c** XRD peaks, of SNC and Ac-SNC nanofiller

to improve the dispersion, matrix-filler interfacial interaction and limit the filler–filler agglomeration among Ac-SNC in PLA [37, 47, 49]. The filler–filler interactions were restricted to a certain extent by surface treatment of the SNC as it decreased the surface energy of the nanofiller [15, 37, 50, 51].

Figure 3a and b shows the TEM images of PLA-SNC-3 wt% and PLA-Ac-SNC-3 wt%, respectively. The optimum concentration of SNC nanofiller in PLA was previously reported to be around 3 wt%, hence this loading was selected for TEM analysis [11, 33]. TEM analysis highlighted the difference in dispersion state of the two nanofillers within the polymer matrix. TEM images for PLA and for PLA-SNC nanocomposites have been reported in previous work [11]. It can be observed that the PLA-SNC-3 wt% had slightly rougher surface than the PLA-Ac-SNC-3 wt%. The rougher and uneven morphology could be due to small agglomerates of SNC in PLA, which was less evident in the case of PLA-Ac-SNC-3 wt%. The Ac-SNC seemed to disperse homogeneously in the nanocomposite; this indicated that acetylation promoted interfacial adhesion at the interface of Ac-SNC and PLA [49, 51].

Oxygen Permeability

Figure 4 shows the reduction in oxygen transmission rate (OTR) values for neat PLA and PLA nanocomposites with SNC and Ac-SNC as nanofiller. An effective barrier to surrounding atmosphere is crucial to avoid fouling or degradation of commodity inside the package through

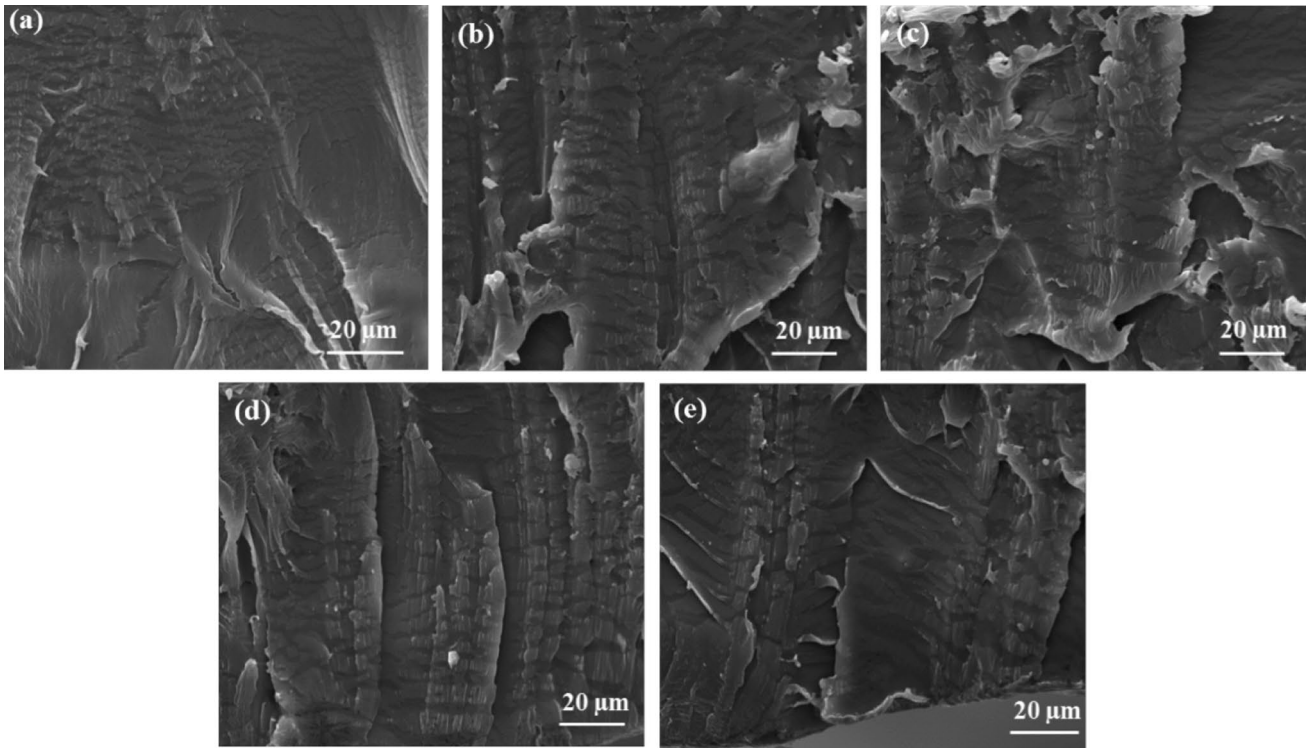

Fig. 2 SEM images of nanocomposites **a** PLA, **b** PLA-SNC-1 wt%, **c** PLA-SNC-3 wt%, **d** PLA-Ac-SNC-1 wt%, and **e** PLA-Ac-SNC-3 wt%

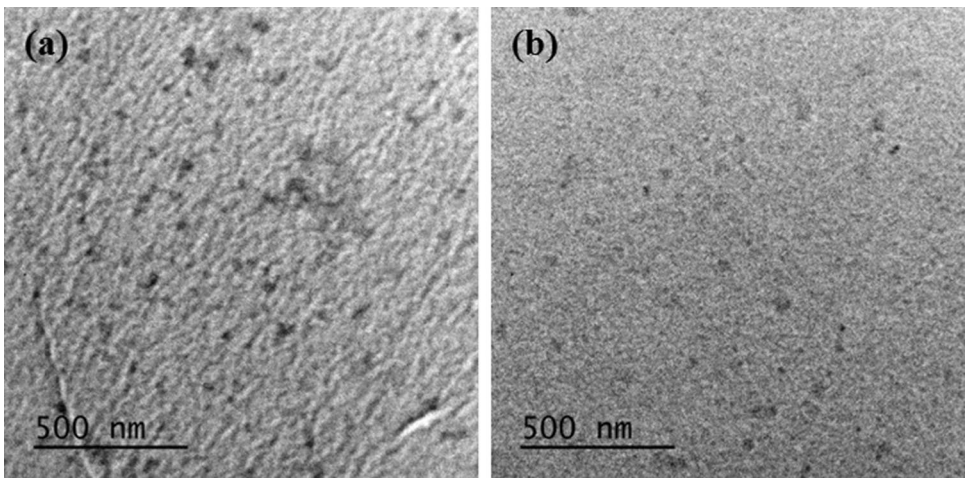

Fig. 3 TEM images of nanocomposites **a** PLA-SNC-3 wt%, and **b** PLA-Ac-SNC-3 wt%

oxidation or humidity, particularly when aiming for food packaging applications [15, 52]. Waxy maize starch (99% amylopectin) by itself has been reported to be an excellent barrier to oxygen [53], and as the SNC used in the current study was obtained from acid hydrolysis of waxy maize starch, it was expected to improve the barrier property of PLA nanocomposite. Additionally, the SNC preparation rendered square-like nano-platelets of SNC [11], which have been reported to create a tortuous pathway hindering the diffusion of the oxygen molecule [10, 26, 54–58].

The improvement in barrier properties was evident for all the nanocomposites as the OTR was less than neat PLA in all cases. However, decrease in oxygen diffusion through the nanocomposite was more pronounced when Ac-SNC was incorporated in PLA than SNC. The improvement in barrier properties confirmed the positive effect of adding either acetylated SNC or unmodified SNC to PLA. Even the PLA nanocomposite with unmodified SNC showed significant improvement in the oxygen barrier property of PLA nanocomposites [47]. This could be attributed to efficient

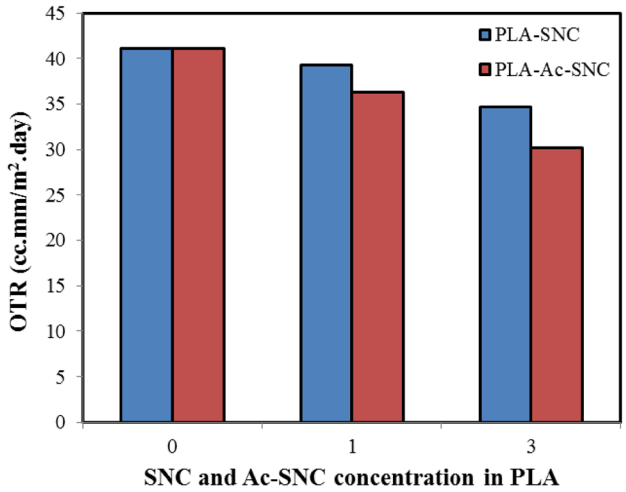

Fig. 4 Oxygen transmission rate of PLA, PLA-SNC and PLA-Ac-SNC nanocomposites

matrix-filler interaction and good dispersion of Ac-SNC, which aided in creating a tortuous diffusive pathway for the entrant oxygen molecule, ultimately delaying the transmission pathway of the penetrant through the nanocomposite film [47].

Mechanical Properties

The results of mechanical properties assessed by tensile tests of neat PLA, PLA-SNC and PLA-Ac-SNC nanocomposites are shown in Fig. 5. The effect of adding the SNC and Ac-SNC on the nanocomposite's mechanical properties, which included tensile strength (σ_b), Young's modulus (E_{Young}), and elongation at break (ε_b) was studied. Although SNC, with various surface modifications, have successfully been used as reinforcement in various polymers, for instance in poly (vinyl alcohol) [59], poly (butylene succinate) [49], polylactic acid [8, 33], natural rubber [25], starch [30, 31, 54, 60–62], pullulan [27], waterborne polyurethane [29, 63], poly(butylmethacrylate) [64], carboxymethyl chitosan [55], and amaranth protein films [57, 65]; acetylated SNC incorporated in PLA has not been reported to date.

The addition of SNC and Ac-SNC resulted in an increase in tensile strength and Young's modulus of all the nanocomposites when compared to neat PLA. Tensile strength measures the capability of the material to bear stress [8]. The reinforcement effect was more pronounced as the nanofiller concentration increased to 3 wt% [66]. The tensile strength was highest for PLA-Ac-SNC-3 wt%, which could be attributed to the enhanced interfacial adhesion and good dispersion of Ac-SNC within the PLA matrix [32, 33, 37, 52]. The trend in the elongation at break values was reversed as the values decreased with the addition of SNC and Ac-SNC when compared to neat PLA. As the reduction in ε_b value was more pronounced in PLA-SNC nanocomposite, this indicated that there was an increased brittleness within the nanocomposite due to the presence of rigid SNC [37, 48]. However, an increase was observed in the PLA-Ac-SNC nanocomposites relative to PLA-SNC nanocomposites. Similar results were reported for PLA nanocomposite with unmodified and modified (surfactant) cellulose nanocrystals [48]. This emphasized the positive effect of acetylation on the nanocomposites.

The values attained by means of tensile testing of nanocomposites confirmed the plasticization effect achieved through surface modification of SNC and the results complemented the morphology results of the nanocomposites [48]. Overall this suggested that the final properties of nanocomposites could be modified as per the requirement of the intended application, based on the concentration and surface modification of SNC, to conform biodegradable nanocomposites. Also, all the filled nanocomposites had slightly better properties than its unfilled counterpart or neat PLA [67].

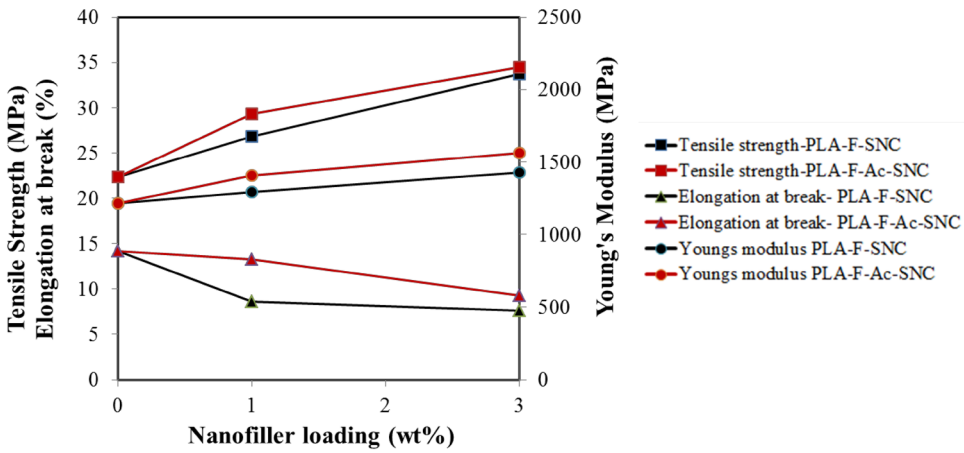

Fig. 5 Mechanical properties of PLA, PLA-SNC and PLA-Ac-SNC nanocomposites

Shear Rheology

The rheological study helps to assess the extent of dispersion of nanofillers within the polymer matrix of a nanocomposite and is considered as a complimentary tool to the traditional characterizations [68, 69]. In the present study the extent of the dispersion of SNC and Ac-SNC in PLA was assessed using the storage modulus, loss modulus and dynamic viscosity data, which was obtained through the dynamic frequency sweep tests of the nanocomposites at 170 °C. Figure 6a compares the storage modulus and dynamic viscosity as function of frequency of PLA-SNC and PLA-Ac-SNC nanocomposites with 0–3 wt% of SNC and Ac-SNC. The significant improvements in the storage modulus of nanocomposites with lower loadings (1–3 wt%) of SNC and Ac-SNC was apparent from Fig. 6a when compared to neat PLA, and the change in storage modulus was more substantial in the lower frequency region. The storage modulus and dynamic viscosity of PLA-Ac-SNC nanocomposites was comparatively higher than the PLA-SNC nanocomposites and was more evident in the low frequency region. This confirmed the positive effect of acetylation which could possibly be due to the uniform dispersion of Ac-SNC within the PLA matrix. This effect was apparent in the low frequency region, due to the low deformation of the nanofiller [70]. The dynamic viscosity curves revealed that the nanocomposite viscosity trend was declining as the frequency increased, displaying non-Newtonian behaviour [71, 72]. In the lower frequency region, the nanocomposites were more solid-like and at higher frequency they were more fluid-like (shear- thinning) [11, 70, 73]. The hydrodynamic forces were more dominant at higher frequencies [74] which led to this behaviour whereas in the low frequency region the rheological parameters were influenced

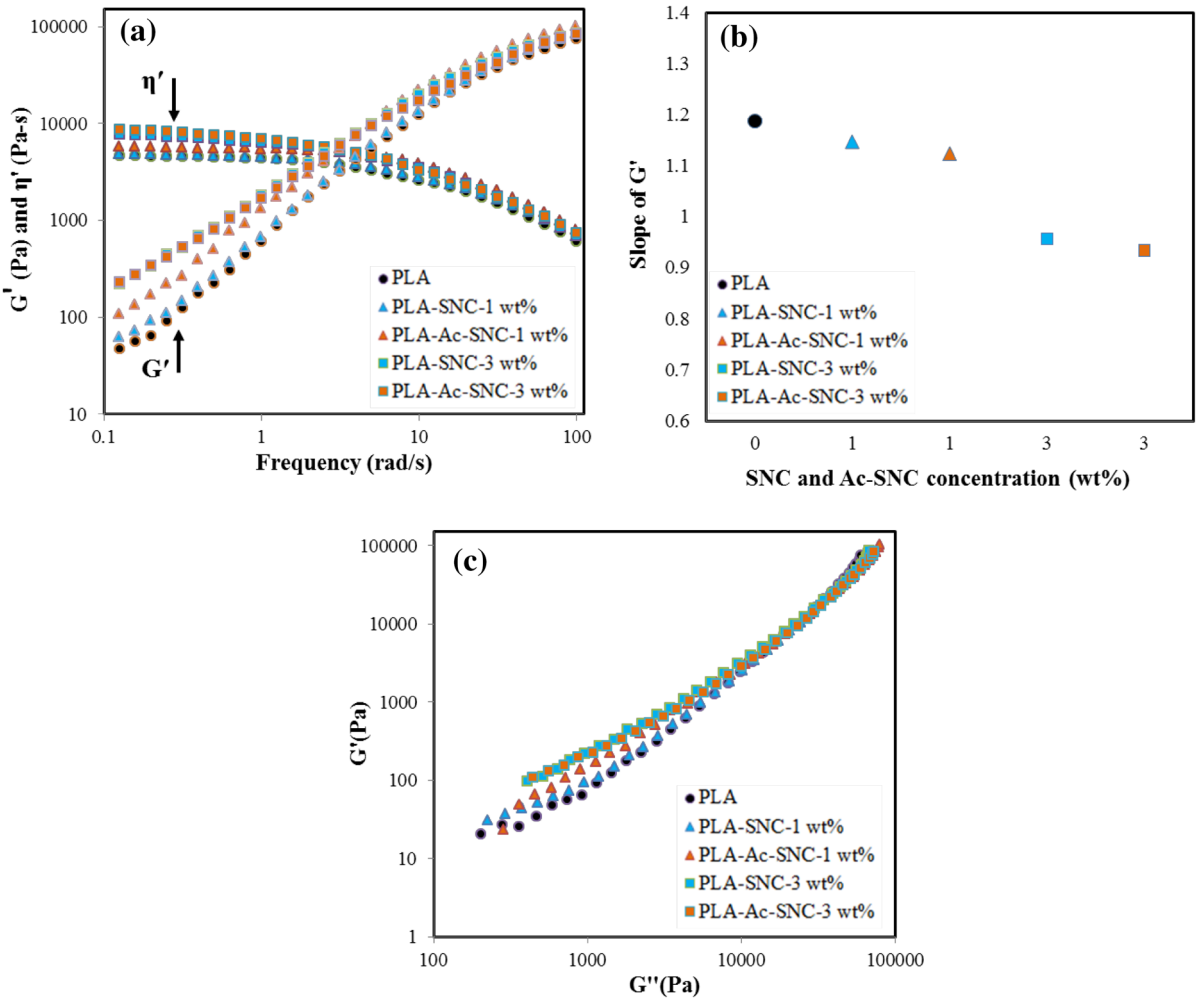

Fig. 6 **a** Storage modulus and dynamic viscosity as a function of frequency of PLA-SNC (Blue) and PLA-Ac-SNC (Orange) nanocomposites, **b** Slope of storage modulus curves at 0–3 wt% SNC (Blue) and Ac-SNC (Orange) loadings, and **c** Plot of G′ versus G″ of PLA-SNC (Blue) and PLA-Ac-SNC (Orange) nanocomposites with 0–3 wt% of SNC and Ac-SNC at 170 °C (Color figure online)

by the Van der Waals interactions among the SNCs [69]. The high frequency data was governed by hydrodynamic forces due to the greater shear rates experienced by PLA confined between the nanofillers [75]. While in the low frequency regions the viscoelastic properties were reliant on the interactions and network structures among the particles. The intention to modify the surface of the SNC by acetylation was to improve the dispersion of these nanofiller within the hydrophobic PLA matrix by restricting the filler–filler interactions and enhancing the matrix-filler interactions. The hydrophilic hydroxyl groups on SNC were replaced to a certain degree by the hydrophobic acetyl group that were more compatible with the PLA matrix, as observed by the improvement in the rheological properties.

Figure 6b shows the slope of storage modulus curves at 0–3 wt% SNC and Ac-SNC loadings. This graph was plotted to estimate the rheological percolation threshold among the prepared set of nanocomposites. It was observed that the minimum slope occurred for PLA-Ac-SNC-3 wt% and this was the most well dispersed nanocomposite as compared to the other formulations. This suggested that Ac-SNC was better nanofiller when compared to SNC in terms of dispersion within the hydrophobic media. A similar trend in results was observed for the barrier and mechanical properties discussed in previous sections. The Hans plot shown in Fig. 6c, a plot of G′ versus G″, confirmed that the slope of the nanocomposites in the low frequency region was dependent on the nanofiller concentration and tended to decrease as the SNC and Ac-SNC concentrations increased. The PLA-Ac-SNC nanocomposites had lower slopes than the PLA-SNC nanocomposites and this could be attributed to the uniform dispersion of the Ac-SNC which led to the formation of a network structure within the PLA matrix [71, 74]. In the high frequency region, the slope of G′ versus G″ was very similar to that of neat PLA as it reached the inflection point. Similar findings were reported for PLA and cellulose nanocrystals (CNC) based nanocomposites by Kamal and Khoshkava [69]; they attributed the change in slope to the change in microstructure of the nanocomposites with the addition of CNCs.

Conclusions

Poly(lactic acid) (PLA) based nanocomposite films, with starch nanocrystals (SNC) and acetylated starch nanocrystals (Ac-SNC) as nanofillers, were prepared and examined for their suitability for packaging applications. The incorporation of SNC and Ac-SNC in PLA had prominent effect on the mechanical and barrier properties of the nanocomposite even at lower loadings of 1 and 3 wt%. With the intention to further enhance the dispersion of SNC in PLA, a surface modification to obtain Ac-SNC was performed. The two nanofiller, SNC and Ac-SNC were incorporated into neat PLA at two different concentrations (1 and 3 wt%) through the solvent casting technique.

The morphological examinations revealed that the PLA-SNC nanocomposites were rougher as compared to the PLA-Ac-SNC nanocomposites, due to better well-dispersed Ac-SNC in PLA. The surface modification created hydrophobic surfaces on Ac-SNC and favoured the dispersion of these nanofiller in PLA matrix. The oxygen permeability and mechanical testing results indicated that both the nanofillers, SNC and Ac-SNC had the potential to improve the oxygen barrier and tensile properties of PLA nanocomposite. As the SNC have square like platelet shape, which created tortuous diffusive paths for penetrant molecules, they were considered as suitable nanofiller for food packaging applications. The rheological investigations underlined the positive effect of surface modification of SNC as the rheological properties were improved for PLA-Ac-SNC nanocomposites compared to PLA-SNC nanocomposites. The current research highlighted the potential of SNC and Ac-SNC as nanofillers to develop sustainable, low-cost and high performance nanocomposites.

Acknowledgements The research work reported in this paper was funded by the RMIT University, Melbourne, VIC 3001, Australia. The authors are grateful to Dr Robert Brkljaca and Sunly Prum from the School of Science, RMIT University for their assistance with NMR, and Mike Allan and Dr Muthu Pannirselvam from the School of Engineering, RMIT University for their assistance with the Mocon and Rheological analysis. The authors acknowledge the facilities, and the scientific and technical assistance of the RMIT University's Microscopy & Microanalysis Facility (RMMF), a linked laboratory of the Australian Microscopy & Microanalysis Research Facility.

References

1. Scaffaro R et al (2017) Polysaccharide nanocrystals as fillers for PLA based nanocomposites. Cellulose 24(2):447–478
2. Arrieta MP et al (2014) Multifunctional PLA-PHB/cellulose nanocrystal films: processing, structural and thermal properties. Carbohyd Polym 107:16–24
3. Auras R, Harte B, Selke S (2004) An overview of polylactides as packaging materials. Macromol Biosci 4(9):835–864
4. Fortunati E et al (2012) Effects of modified cellulose nanocrystals on the barrier and migration properties of PLA nano-biocomposites. Carbohyd Polym 90(2):948–956
5. Kasa SN, Omar MF, Ismail IN (2017) Characterization and properties of acetylated nanocrystalline cellulose (aNC) reinforced polylactic acid (PLA) polymer. AIP Conf Proc 1901(1):030014
6. Spinella S et al (2015) Modification of cellulose nanocrystals with lactic acid for direct melt blending with PLA. 1664: 070019
7. Mukherjee T et al (2017) Chemically imaging the interaction of acetylated nanocrystalline cellulose (NCC) with a polylactic acid (PLA) polymer matrix. Cellulose 24(4):1717–1729
8. Yu J et al (2008) Structure and mechanical properties of poly(lactic acid) filled with (starch nanocrystal)-graft -poly(ε -caprolactone). Macromol Mater Eng 293(9):763–770

9. Garcia NL et al (2012) Biodegradable materials from grafting of modified PLA onto starch nanocrystals. Polym Degrad Stab 97(10):2021–2026
10. Espino-Pérez E et al (2016) Nanocomposites with functionalised polysaccharide nanocrystals through aqueous free radical polymerisation promoted by ozonolysis. Carbohyd Polym 135:256–266
11. Takkalkar P et al (2018) Preparation of square-shaped starch nanocrystals/polylactic acid based bio-nanocomposites: morphological, structural, thermal and rheological properties. Waste Biomass Valor. https://doi.org/10.1007/s12649-018-0372-0
12. Singh AA et al (2018) Synergistic effect of chitin nanocrystals and orientations induced by solid-state drawing on PLA-based nanocomposite tapes. Compos Sci Technol 162:140–145
13. Pal AK, Katiyar V (2016) Nanoamphiphilic chitosan dispersed poly (lactic acid) bionanocomposite films with improved thermal, mechanical, and gas barrier properties. Biomacromol 17(8):2603–2618
14. Pal AK et al (2017) Chemomechanical, morphological, and rheological studies of chitosan-graft-lactic acid oligomer reinforced poly(lactic acid) bionanocomposite films. J Appl Polym Sci 135:45546
15. Arrieta MP et al (2015) Bionanocomposite films based on plasticized PLA–PHB/cellulose nanocrystal blends. Carbohyd Polym 121(Supplement C):265–275
16. Herrera N et al (2016) Plasticized polylactic acid nanocomposite films with cellulose and chitin nanocrystals prepared using extrusion and compression molding with two cooling rates: effects on mechanical, thermal and optical properties. Compos A Appl Sci Manuf 83:89–97
17. Sungsanit K et al (2010) Physical and rheological properties of plasticized linear and branched PLA. Korea-Aust Rheol J 22(3):187–195
18. Sungsanit K, Kao N, Bhattacharya S (2012) Properties of linear poly (lactic acid)/polyethylene glycol blends. Polym Eng Sci 52(1):108–116
19. Petinakis E et al (2010) Biodegradation and thermal decomposition of poly(lactic acid)-based materials reinforced by hydrophilic fillers. Polym Degrad Stab 95(9):1704–1707
20. Fortunati E et al (2012) New multifunctional poly(lactide acid) composites: mechanical, antibacterial, and degradation properties. J Appl Polym Sci 124(1):87–98
21. Tolstoguzov V (2004) Why are polysaccharides necessary? Food Hydrocolloids 18(5):873–877
22. Rong SY, Mubarak NM, Tanjung FA (2017) Structure-property relationship of cellulose nanowhiskers reinforced chitosan biocomposite films. J Environ Chem Eng 5(6):6132–6136
23. Wei B et al (2014) Surface chemical compositions and dispersity of starch nanocrystals formed by sulfuric and hydrochloric acid hydrolysis. PLoS ONE 9(2):e86024
24. Zhang G et al (2018) Crystallization of green poly (ε-caprolactone) nanocomposites with starch nanocrystal: the nucleation role switching of starch nanocrystal with its surface acetylation. Ind Eng Chem Res 57(18):6257–6264
25. Angellier H, Molina-Boisseau S, Dufresne A (2005) Mechanical properties of waxy maize starch nanocrystal reinforced natural rubber. Macromolecules 38(22):9161–9170
26. Angellier H et al (2005) Processing and structural properties of waxy maize starch nanocrystals reinforced natural rubber. Macromolecules 38(9):3783–3792
27. Kristo E, Biliaderis CG (2007) Physical properties of starch nanocrystal-reinforced pullulan films. Carbohyd Polym 68(1):146–158
28. Zheng H et al (2009) Structure and properties of starch nanocrystal-reinforced soy protein plastics. Polym Compos 30(4):474–480
29. Chen G et al (2008) Simultaneous reinforcing and toughening: new nanocomposites of waterborne polyurethane filled with low loading level of starch nanocrystals. Polymer 49(7):1860–1870
30. Angellier H et al (2006) Thermoplastic starch—waxy maize starch nanocrystals nanocomposites. Biomacromol 7(2):531–539
31. Piyada K, Waranyou S, Thawien W (2012) Mechanical, thermal and structural properties of rice starch films reinforced with rice starch nanocrystals. Int Food Res J 20(1):439–449
32. Xu C, Chen C, Wu D (2018) The starch nanocrystal filled biodegradable poly(ε-caprolactone) composite membrane with highly improved properties. Carbohyd Polym 182:115–122
33. Yin Z et al (2015) Preparation and properties of cross-linked starch nanocrystals/polylactic acid nanocomposites. Int J Polym Sci 2015:5
34. Shanmugarajah B et al (2019) Valorization of palm oil agro-waste into cellulose biosorbents for highly effective textile effluent remediation. J Clean Prod 210:697–709
35. Yee MJ et al (2018) Synthesis of polyvinyl alcohol (PVA) infiltrated MWCNTs buckypaper for strain sensing application. Sci Rep 8(1):17295
36. Jun LY et al (2019) Immobilization of peroxidase on functionalized MWCNTs-buckypaper/polyvinyl alcohol nanocomposite membrane. Sci Rep 9(1):2215
37. Lin N et al (2011) Surface acetylation of cellulose nanocrystal and its reinforcing function in poly(lactic acid). Carbohyd Polym 83(4):1834–1842
38. Robles E et al (2015) Surface-modified nano-cellulose as reinforcement in poly(lactic acid) to conform new composites. Ind Crops Prod 71:44–53
39. Angellier H et al (2004) Optimization of the preparation of aqueous suspensions of waxy maize starch nanocrystals using a response surface methodology. Biomacromol 5(4):1545–1551
40. Xu Y et al (2010) Preparation and characterization of organic-soluble acetylated starch nanocrystals. Carbohyd Polym 80(4):1078–1084
41. Xiao H et al (2016) Acetylated starch nanocrystals: preparation and antitumor drug delivery study. Int J Biol Macromol 89:456–464
42. LeCorre D, Bras J, Dufresne A (2011) Influence of botanic origin and amylose content on the morphology of starch nanocrystals. J Nanopart Res 13(12):7193–7208
43. Wang YJ, Wang L (2002) Characterization of acetylated waxy maize starches prepared under catalysis by different alkali and alkaline-earth hydroxides. Starch-Stärke 54(1):25–30
44. Putaux J-L et al (2003) Platelet nanocrystals resulting from the disruption of waxy maize starch granules by acid hydrolysis. Biomacromol 4(5):1198
45. Jonoobi M et al (2012) A comparison of modified and unmodified cellulose nanofiber reinforced polylactic acid (PLA) prepared by twin screw extrusion. J Polym Environ 20(4):991–997
46. Nizamuddin S et al (2019) Synthesis and characterization of polylactide/rice husk hydrochar composite. Sci Rep 9(1):5445
47. Fortunati E et al (2012) Effects of modified cellulose nanocrystals on the barrier and migration properties of PLA nano-biocomposites. Carbohyd Polym 90(2):948–956
48. Fortunati E et al (2015) Processing of PLA nanocomposites with cellulose nanocrystals extracted from *Posidonia oceanica* waste: innovative reuse of coastal plant. Ind Crops Prod 67:439–447
49. Lin N et al (2011) Poly(butylene succinate)-based biocomposites filled with polysaccharide nanocrystals: structure and properties. Polym Compos 32(3):472–482
50. Kargarzadeh H et al (2018) Recent developments in nanocellulose-based biodegradable polymers, thermoplastic polymers, and porous nanocomposites. Prog Polym Sci 87:197
51. Zhang G et al (2018) Green poly (β-hydroxybutyrate)/starch nanocrystal composites: tuning the nucleation and spherulite

morphology through surface acetylation of starch nanocrystal. Carbohyd Polym 195:79–88
52. Arrieta MP et al (2014) PLA-PHB/cellulose based films: mechanical, barrier and disintegration properties. Polym Degrad Stab 107:139–149
53. Cazón P et al (2017) Polysaccharide-based films and coatings for food packaging: a review. Food Hydrocolloids 68(Supplement C):136–148
54. Garcia NL et al (2009) Physico-mechanical properties of biodegradable starch nanocomposites. Macromol Mater Eng 294(3):169–177
55. Duan B et al (2011) Preparation and properties of starch nanocrystals/carboxymethyl chitosan nanocomposite films. Starch-Stärke 63(9):528–535
56. LeCorre D et al (2014) All starch nanocomposite coating for barrier material. J Appl Polym Sci. https://doi.org/10.1002/app.39826
57. Condés MC et al (2018) Composite and nanocomposite films based on amaranth biopolymers. Food Hydrocolloids 74(Supplement C):159–167
58. Huang F-Y et al (2015) Preparation and properties of cellulose laurate (CL)/starch nanocrystals acetate (SNA) bio-nanocomposites. Polymers 7(7):1331–1345
59. Chen Y et al (2008) Comparative study on the films of poly(vinyl alcohol)/pea starch nanocrystals and poly(vinyl alcohol)/native pea starch. Carbohyd Polym 73(1):8–17
60. Viguie J, Molina-Boisseau S, Dufresne A (2007) Processing and characterization of waxy maize starch films plasticized by sorbitol and reinforced with starch nanocrystals. Macromol Biosci 7(11):1206–1216
61. Li X et al (2015) Mechanical, barrier and morphological properties of starch nanocrystals-reinforced pea starch films. Carbohyd Polym 121:155–162
62. Ren L et al (2016) Performance improvement of starch films reinforced with starch nanocrystals (SNCs) modified by cross-linking. Starch/Staerke 69:1600025
63. Chang PR et al (2008) Effects of starch nanocrystal-graft-porycaprolactone on mechanical properties of waterborne polyurethane-based nanocomposites. J Appl Polym Sci 111(2):619–627
64. Bel Haaj S et al (2016) Starch nanocrystals and starch nanoparticles from waxy maize as nanoreinforcement: a comparative study. Carbohyd Polym 143:310
65. Condes MC et al (2015) Amaranth protein films reinforced with maize starch nanocrystals. Food Hydrocolloids 47:146–157
66. Yan M, Li S, Zhang M, Li C, Dong F, Li W (2013) Characterization of surface acetylated nanocrystalline cellulose by single-step method. BioResources 8:6330
67. Bondeson D, Oksman K (2007) Polylactic acid/cellulose whisker nanocomposites modified by polyvinyl alcohol. Compos A Appl Sci Manuf 38(12):2486–2492
68. Zhao J, Morgan AB, Harris JD (2005) Rheological characterization of polystyrene–clay nanocomposites to compare the degree of exfoliation and dispersion. Polymer 46(20):8641–8660
69. Kamal MR, Khoshkava V (2015) Effect of cellulose nanocrystals (CNC) on rheological and mechanical properties and crystallization behavior of PLA/CNC nanocomposites. Carbohyd Polym 123:105–114
70. Mukherjee T et al (2013) Improved dispersion of cellulose microcrystals in polylactic acid (PLA) based composites applying surface acetylation. Chem Eng Sci 101:655–662
71. Gupta A et al (2017) Rheological and thermo-mechanical properties of poly(lactic acid)/lignin-coated cellulose nanocrystal composites. ACS Sustain Chem Eng 5(2):1711–1720
72. Narimissa E et al (2015) The comparison between the effects of solvent casting and melt intercalation mixing processes on different characteristics of polylactide-nanographite platelets composites. Polym Eng Sci 55(7):1560–1570
73. Kashi S et al (2018) Phase transition and anomalous rheological behaviour of polylactide/graphene nanocomposites. Compos B Eng 135:25–34
74. Mukherjee T et al (2014) Dispersion study of nanofibrillated cellulose based poly(butylene adipate-co-terephthalate) composites. Carbohyd Polym 102:537–542
75. Sabzi M et al (2013) Graphene nanoplatelets as poly(lactic acid) modifier: linear rheological behavior and electrical conductivity. J Mater Chem A 1(28):8253–8261